WETTING ANGLES MEASURED BY A NON-CONTACT SCANNING PROBE TECHNIQUE, AT THE MICRO- AND NANOSCALE

Antoniu Moldovan, Daniela Buzatu, Marian Bota, IulianBoerasu, Dionezie Bojin, and Marius Enachescu
Center for Surface Science and NanoTechnology, University "Politehnica" of Bucharest;
Splaiul Independentei 313, Bucharest 060042, Romania
marius.enachescu@upb.ro

Abstract: We report about the implementation of a truly non-contact scanning probe technique, Scanning Polarization Force Microscopy(SPFM), suitable for the investigation of surface properties of soft and liquid samples. The technique is based on the measurement and control of the electrostatic polarization force between a conductive AFM tip and the sample. SPFMallowed the measurement of topography profiles of micro- and nano-droplets of glycerol on silicon and silicon dioxide. Contact angle values were calculated from these topography profiles in order to investigate the wetting properties at the microscopic scale.

1. Introduction

Atomic Force Microscopy (AFM) and related techniques of the Scanning Probe Microscopy (SPM) family allow the reconstruction of the topography of the surfaces of solid materials with sub-nanometer lateral resolution and sub-Ångström vertical resolution. The ability to visualize the 3D contour of the surface of droplets or layers of liquid offers advantages in numerous applications (study of lubricants, surfactants, mechanisms and effects of corrosion etc.) [1].

Scanning Polarization Force Microscopy (SPFM), a relatively new technique, was first implemented at Lawrence Berkeley National Laboratory [2] and represents an extension of Atomic Force Microscopy. It offers a new way to investigate surface properties such as topography of very soft or even liquid surfaces, microscopic contact angle, dielectric constant, etc. which are not accessible viaother surface characterization techniques.

The SPFM technique is based on the measurement of the electrostatic polarization force between a conductive sharp tip and the investigated surface. The intense electric field surrounding the tip apex creates a local accumulation of electric charge on the sample surface for conductive materials and a local increase of the electric polarization for dielectric materials. The polarization force acting on the tip will cause a proportional bending of the cantilever. The bending can be measured by the laser lever detection technique employed in usual AFM experiments (Figure 1): a laser light is reflected off the back of the cantilever and falls on a position sensitive photo-detector (PSPD). The output signal of the detector is proportional to the bending of the cantilever and, consequently, has the same time dependence as the polarization force.

If the polarization bias has a DC component (V_{DC}) and an AC component of the form $V_{tip}\sin(\omega t)$, and the local surface potential is V_{surf} the net bias between tip and sample will be$V(t) = V_{DC} - V_{surf} + V_{tip}\sin(\omega t)$ and, by the coarse approximation of the tip-surface system with a parallel plate capacitor, the electrostatic force will be:

$$F(t) = \frac{C}{d}\left[(V_{DC} - V_{surf})^2 + \frac{1}{2}V_{tip}^2\right] + 2\frac{C}{d}(V_{DC} - V_{surf})V_{tip}\sin(\omega t) - \frac{1}{2}\frac{C}{d}V_{tip}^2\cos(2\omega t)$$

As can beseen, the electrostatic force has three terms with different time-dependencies:$F_{0\omega}$,$F_{\omega}$and $F_{2\omega}$. The PSPD signal will have the same time dependence as the polarization force and the three components of the signal, 0ω, 1ω and 2ω will be separated by a lock-in technique (Figure 1). The topography of the surface is reconstructed from the signal which drives the vertical elongation of the scanner in order to maintain constant amplitude of the 2ω signal during scanning.

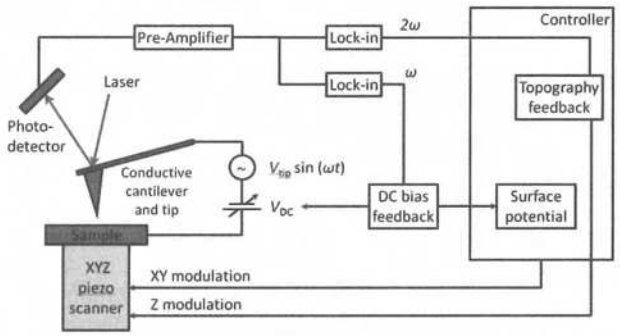

Figure 1: Detection and feedback mechanism in SPFM

In order to analyze the size, shape and behavior of glycerol nano-droplets on different substrates we used the effect of long-range forces on the structure and wetting properties of liquids films, similar to the approach of de Gennes [3]. By minimization of the free energy G, the shape $z(r)$ of a liquid drop on a solid surface can be obtained. For a circularly symmetric drop the free energy can be written as an integral over the area covered by the drop:

$$G = G_0 + \int_{drop} 2\pi r\,dr\left[-S + \frac{\gamma}{2}\left(\frac{dz}{dr}\right)^2 + P(z) - \frac{\mu_{vapor} - \mu_{liq}}{v_{mol}}\cdot z\right] \quad (1)$$

where the first term: $S = \gamma_{sv} - \gamma_{sl} - \gamma$ is the spreading coefficient, which characterizes the wetting properties of a surface by a given liquid at short ranges; if $S>0$, the liquid will wet the surface, and if $S< 0$, a contact angle will exist, determined by Young's equation $\gamma \cos\theta = \gamma_{sv} - \gamma_{sl}$; γ_{sv} is the solid-vapor surface energy; γ_{sl} is the solid-liquid surface energy; γ is the liquid-vapor surface energy. The second term is due to the excess surface because of the curvature of the drop and is valid for the case of shallow drops. The third term $P(z)$ is the surface potential energy between the surfaces, the energy needed to create a unit area of surface or interface. The last term describes the supersaturation in terms of chemical potentials of the vapor and liquid; v_{mol} is the molecular volume of the liquid [3].

By minimization of G in eq. (1) under constant volume of droplet $V = \int z(r)\, 2\pi r\, dr$ and assuming a spherical cap shape of the droplets [4], it gives for $z \to 0$ (near the base of the drop) that the relation between the effective contact angle θ and the disjoining pressure $\Pi(e) = -\frac{dP}{de} = -P'(e)$ [5] is:

$$\theta^2 = \theta_0^2 + \frac{2}{\gamma}[P(e) + e\Pi(e)], \qquad (2)$$

where e is the height of the droplet; $\theta_0^2 = -\frac{2}{\gamma}P(0)$ is the macroscopic contact angle squared.The contact angle θ depends on the interfacial energies and is influenced by the disjoining pressure. The disjoining pressure is related to the spreading coefficient S by:

$$S = \int_0^\infty \Pi(x)\, dx = P(e)_{e\to 0} \qquad (3)$$

Eq.(2) can be transformed into the following relation:

$$P(e) - eP'(e) = (\theta^2 - \theta_0^2)\frac{\gamma}{2} \qquad (4)$$

Thus, using the dependence described in eq. (4), the potential energy $P(e)$between the surfaces can be determined after measuring the dependence of contact angle on droplet height. Scanning polarization force microscopy, implemented recently in our laboratory, was chosen to investigate the contact angle and disjoining pressure of glycerol on Si, SiO_2 covered Si (native SiO_2) and bulk SiO_2, as the only technique able to offer nanometer resolution for measuring the shapes of micro- and nano-droplets.

2. Experimental

Substrate preparation

The substrates were bare silicon, silicon covered with native oxide and bulk silicon oxide, cut in squares of ~10×10 mm^2. They were washed in an ultrasonic bath for several cycles in ultrapure water and acetone, for the removal of organic contaminants and debris resulting from the cutting process. In order to expose the bare silicon (remove the native oxide layer), silicon substrates were immersed for one minute in a dilute solution of HF (20% wt.).

Upon examination with the optical microscope, the surface of the substrates appeared free of defects and impurities over large areas.

Deposition of micro- and nano-droplets

Glycerol droplets were created on the substrates by condensation: the substrates were held upside down inside a Berzelius glass containing heated glycerol, at a height of ~5mm from the liquid surface. After a few seconds the surface of the substrates achieved a "foggy" appearance, which proved the presence of microscopic droplets. This was confirmed by further optical microscopy inspection (Figure 2).

Optical microscopy

Optical microscopy images were recorded using an Olympus upright optical microscope, with its ×100 objective.

The images in Figure 2 show typical distributions of glycerol droplets on the substrates. For the same deposition time, glycerol condenses in a relatively dense distribution of small droplets on silicon, whereas on native SiO_2 and bulk SiO_2 it forms larger and more distant droplets. This could be attributed to the nanoscale roughness of the bare silicon surface, caused by the wet etching process. The droplets become pinned to the atomic defects, preventing the coalescence of small droplets into bigger droplets.

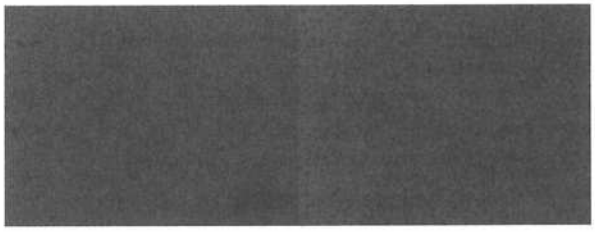

(a) (b)

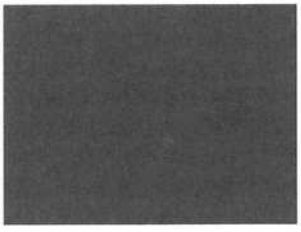

(c)

Figure 2: Optical microscopy images of the samples after the deposition of the nano-droplets: a) glycerol on Si; b) glycerol on native SiO_2; c) glycerol on bulk SiO_2. Field of view ~70μm × 55μm

SPFM analysis

The SPFM measurements were conducted in ambient air (room temperature, RH ~50%) on a modified home-built AFM system controlled by commercial electronics (RHK

SPM100 and PLLPro2). The samples were placed on steel carriers which were electrically connected to the ground of the system. SPFM measurements were carried out in AC mode, with a bias of 3-5 V amplitude and 3 kHz frequency applied between the conductive tip and ground. Commercial conductive coated (Pt and Cr/Au), contact mode silicon tips were used for the measurements (Mikromasch, Nanosensors, AppNano). The nominal spring constant of the cantilevers was less than 1 N/m.

Figure 3 shows typical SPFM-AC topography images of the samples after the deposition of the droplets on Si, native SiO_2 and bulk SiO_2. The deposited droplets have shapes close to spherical caps, which allows us to use the de Gennes theoretical model [3] in order to determine the surface potential energy $P(e)$ between glycerol and Si and SiO_2.

Droplet profiles were extracted from the SPFM topography images taken on the samples, by plotting the height versus lateral displacement along horizontal segments taken across the point of maximum height for each chosen droplet. Some of the profiles are plotted in Figure 4.

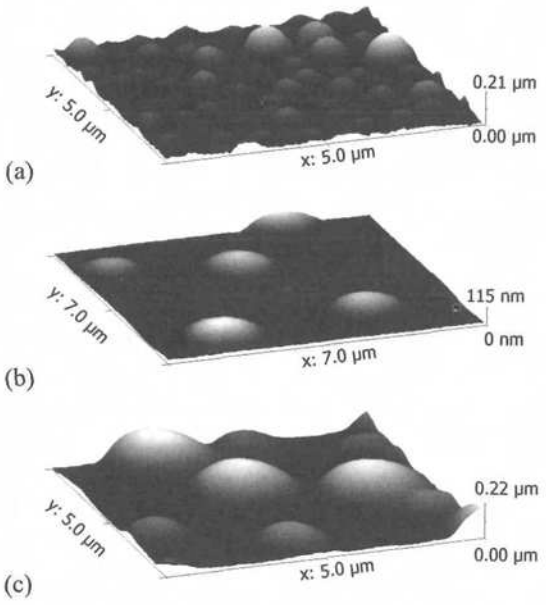

Figure 3: Typical SPFM-AC images of the samples after the deposition of the droplets: a) glycerol on Si, 5µm × 5µm; b) glycerol on native SiO_2, 7µm × 7µm; c) glycerol on bulk SiO_2, 5µm × 5µm

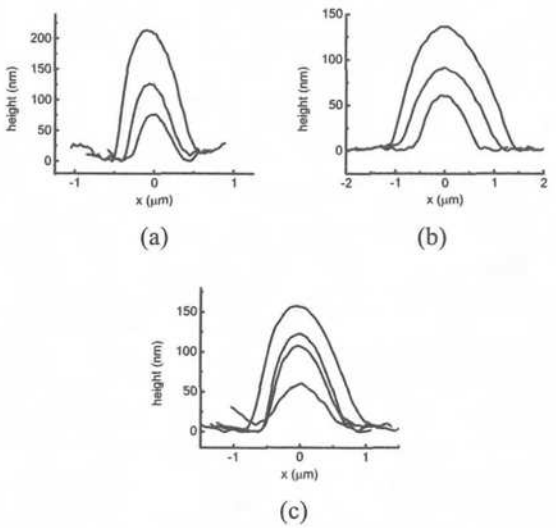

Figure 4: Line-cut profiles of droplets of glycerol on: a) silicon; b) native SiO_2; c) bulk SiO_2

3. Results and discussions

Contact angle measurements

For a macroscopic liquid droplet the contact angle is defined as the angle at which the surface of the liquid meniscus meets the surface of the substrate, measured through the liquid – as shown in Figure 5a.

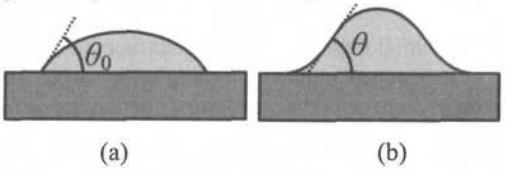

Figure 5: Schematic drawing of the contact angle for the case of: a) macroscopic droplet, b) microscopic droplet

For micro- and nano-droplets, as shown in Figure 4 and Figure 5b, the liquid meniscus does not meet the solid surface at a precise angle and the graph of the line-cut profile has two inflection points (one on each side of the section). In this case the contact angle is calculated by measuring the slope (first derivative) of the line-cut profile at these inflection points [1]. Contact angle values corresponding to the droplets shown in Figure 2 were plotted as a function of droplet height (Figure 6).

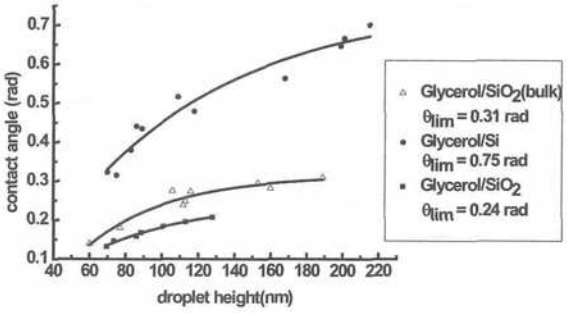

Figure 6: Dependence of contact angle on droplet height for glycerol on silicon, native SiO_2 and bulk SiO_2

Potential energy determination

Using relation $\theta^2 = \theta_0^2 + \frac{2}{\gamma}[P(e) + e\Pi(e)]$ and the dependence of contact angle on droplet height (Figure 6) we calculate the dependence of surface potential energy $P(e)$ between the interfaces for glycerol on Si, glycerol on native SiO_2 and glycerol on bulk SiO_2. The results are shown in Figure 7. The macroscopic contact angle θ_0 was determined as an exponential fitting parameter for the microscopic contact angle dependencies.

The contact angle of glycerol on Si, native SiO_2 and bulk SiO_2 varies with height as shown in Figure 6. The decrease of the contact angle with decreasing droplet height indicates that the surface potential $P(e)$ is negative and an exponential dependence $P(e) = P_0 \exp(-\frac{e}{\delta})$ [4] with distance gives a good fit (Figure 7), were P_0 and δ are the fitting parameters. From the fitting parameters we determined the dependence of the potential energy on droplet height:

$$P(e) = -28 \cdot 10^{-3} \exp(-e/107\ \text{nm})\ \text{J/m}^2$$

for glycerol on silicon;

$$P(e) = -4 \cdot 10^{-3} \exp(-e/60.5\ \text{nm})\ \text{J/m}^2$$

for glycerol on native SiO_2;

$$P(e) = -8 \cdot 10^{-3} \exp(-e/52\ \text{nm})\ \text{J/m}^2$$

for glycerol on bulk SiO_2.

The exponential dependence of the surface potential energy $P(e)$ with distance indicates hydrophobic attractive forces between glycerol and the substrates, characterized by decay lengthsδ = 107 nm for glycerol on silicon, δ = 60.5 nm for glycerol on native SiO_2 and δ = 52 nm for glycerol on bulk SiO_2.

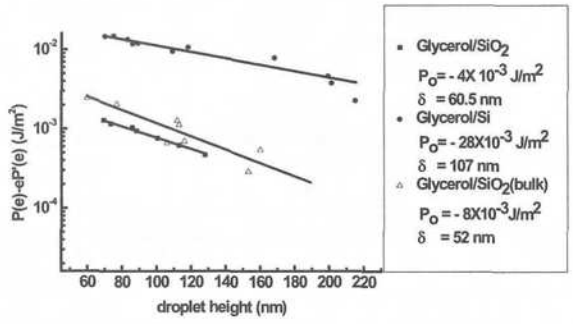

Figure 7: Semilog plot of $P(e)$–$eP'(e)$ vs. e, the droplet height, for glycerol on Si, native SiO_2 and bulk SiO_2

In our calculations we have used the value 64 mJ/m^2 for the surface tension for glycerol.

The strength of the potential at e = 0 nm gives the spreading coefficient S for each case:

$$S = P(0) = -28 \cdot 10^{-3}\ \text{J/m}^2$$

for glycerol on silicon;

$$S = P(0) = -4 \cdot 10^{-3}\ \text{J/m}^2$$

for glycerol on native SiO_2;

$$S = P(0) = -8 \cdot 10^{-3}\ \text{J/m}^2$$

for glycerol on bulk SiO_2.

In all these casesthe values for spreading coefficient indicate a weak hydrophobic interaction by comparison with surface tension of glycerol. These potential energies give a negative disjoining pressure Π of 2.8 atm for glycerol on Si, 0.6 atm for glycerol on native SiO_2 and 1.5 atm for glycerol on bulk SiO_2at e close to zero.

4. Conclusions

We have successfully implemented the SPFM technique for the study of the wetting properties of glycerol on silicon, native SiO_2 and bulk SiO_2at the micro and nanoscale. SPFM has demonstrated its usefulness in studies of wetting properties by measuring the shape of sub-micrometer size liquid droplets on surfaces.The recorded SPFM topography images of the droplets allowed the direct determination of the microscopic contact angle. The decrease of microscopic contact angle with droplet height was observed, which is an indication that the surface potential $P(e)$ is negative and has an exponential dependence. The dependence of $P(e)$ on droplet height, the spreading coefficient (S< 0) and the disjoining pressure Π were calculated, giving information about the strength of the force between the liquid/air and liquid/substrate interfaces.

Acknowledgments

The authors acknowledge the financial support of the European Union and the Romanian Government, received through grants POSDRU/107/1.5/S/76813 and POSCCE-O212-2009-2/12689/717.

References

[1]Salmeron M. *Nanoscale wetting and de-wetting of lubricants with Scanning Polarization Force Microscopy*. Fundamentals of Tribology and Bridging the Gap Between the Macro- and Micro/Nanoscales, NATO Science Series Volume 10, 2001, 651

[2]Hu J, Xiao XD, Ogletree DF, Salmeron M. *Imaging the condensation and evaporation of molecularly thin films of water with nanometer resolution*, Science 268, 1995

[3]de Gennes PG. *Wetting: statics and dynamics*. Rev.Mod.Phys. 57 827, 1985

[4]Xu L, Salmeron M. *Scanning Polarization Force Microscopy Study of the Condensation and Wetting Properties of Glycerol on Mica*. J.Phys.Chem. B 102 7210, 1998

[5]Derjaguin BV, Churaev NV, Muller VM, Kitchener JA.*Surface Forces*. Consultants Bureau, New York, 1987